Transformation Temperatures and Electrochemical behavior of Polycrystalline Fe-Doped Ni-Mn-Ga and Co-Ni-Ga Alloys

M. Sanchez-Carrillo[1], J.P. Flores-de los Rios[2,], C.G. Nava-Dino[2], H. Flores-Zuñiga[3], R. Narro-Garcia[2], M.C. Maldonado-Orozco[2], F.H. Estupiñan-Lopez[4], J.G. Chacon-Nava[5]*

[1] Universidad Tecnológica de Chihuahua Sur, km 3 Carretera Chihuahua a Aldama S/N, C.P. 31313, Chihuahua, Chih., México.
[2] Universidad Autónoma de Chihuahua, Facultad de Ingeniería, Circuito Universitario Campus 2 S/N, C.P. 31125, Chihuahua, Chih., México.
[3] División de Materiales Avanzados, Instituto Potosino de Investigación Científica y Tecnológica A. C., Camino a la Presa de San José # 2055. Lomas 4a. Secc. 78216 San Luis Potosí, S.L.P. México.
[4] Universidad Autónoma de Nuevo León, Facultad de Ingeniería Mecánica y Eléctrica, Centro de Investigación e Innovación en Ingeniería Aeronáutica, C.P. 66455, San Nicolás de los Garza, Nuevo León, México
[5] Departamento de Metalurgia e Integridad Estructural, Centro de Investigación en Materiales Avanzados, S.C., Miguel de Cervantes 120, Complejo Industrial Chihuahua, C.P. 31136, Chihuahua, Chih., México.
[*]E-mail: jpdelosrios@uach.mx

The effect of *Fe* addition on martensitic transformation temperatures and electrochemical behavior was studied in polycrystalline $Ni_{51.4}Mn_{24.8-X}Ga_{23.8}Fe_X$ alloys (*1<x<2.2*) and $Co_{38.3}Ni_{32.1}Ga_{29.6}$ as alternative to *Ni-Mn-Ga* alloys which are used as ferromagnetic shape memory alloys. The analysis of corrosion rates was conducted by cyclic polarization curves with potentiostat-galvanostat equipment. The corrosion morphologies were also analyzed by scanning electron microscopy (*SEM*). The kinetics of corrosion was found to decrease with increasing *Fe* content in the alloy, while the martensitic transformation temperatures increased with increasing *Fe* content. The $Co_{38.3}Ni_{32.1}Ga_{29.6}$ alloy shows i_{corr} lower than the *Ni-Mn-Ga* alloy. From results, the studied alloys exhibited a general dissolution in the anodic branch where a spontaneous passive zone occurred at certain potential and some elements like Co, Mn and also Ni were present in a higher percentage in corrosion deposits.

1. INTRODUCTION

Alloys of the system *Ni-Mn-Ga* are type Heusler structure alloys. These alloys exhibit a martensitic transformation which is related to the shape memory effect. Since the discovery of large strains (up to 10%) induced by the magnetic field in the ferromagnetic alloys, has been of growing interest in the development and/or research of these type of alloys due to the wide range of potential applications [1, 2] . Some of its applications of the mentioned alloys are actuators, MEM´s [3] strain sensors [4] or vibration dampers [5]. The interest of Ni-Mn-Ga systems is that the alloys show an important response due to external stimuli at some temperatures close to martensitic transition. Magnetic field is an effective stimuli to induce a transition, increasing the deformation and changes in magnetization [6]. The changes on this kind of alloys provide fascinating properties to this materials, such as elastocaloric [7] and magnetocaloric effect [8] rising the interest for applications in solid state cooling near to the room temperature [9]. Nevertheless, the fragility is a limiting factor for practical applications of these materials. Cherechukin et al [10] reported that low doping of *Fe* in *Ni-Mn-Ga* alloys enhancing the toughness of the material without sacrificing magnetic and thermoelastic properties. The structure, shape memory effect, changes in magnetic properties and Curie temperatures of *Ni-Mn-Ga* alloys doped with *Fe* has been studied [10-18].

Investigations of alternatives for ferromagnetic shape memory applications has been carried out: *Fe–Pd* [19], *Fe–Pt* [20], *Ni–Mn–Al* [21], and *Co–Ni–Al* [22, 23] because the necessity of improve the high brittleness of *Ni-Mn-Ga* alloys. Alloys like, *Ni–Fe–Al* [24] and *Co–Ni–Ga* [25] have been considered as a good candidates that response to a magnetic stimuli, specially for the presence of a γ phase (disordered FCC) improving ductility in these materials [26, 27], however, high percentage of this phase can cause a decrease of strain properties by magnetic field. Contrary to *Ni–Mn–Ga* alloys, *Co-* and *Ni-*based alloys present dual-phase structures. Similar behavior was also found in *Co–Ni–Al* [26], *Ni–Al–Fe* [28] and *Ni–Fe–Ga* [29].

Since under application conditions of ferromagnetic shape memory alloys that shows changes of shape, corrosion protection with coatings would be difficult. Hence, these alloys have to exhibit high resistance to corrosion attack. Nevertheless, up to date corrosion studies of *Co-Ni-Ga* alloys are still scarce and studies of *Ni-Mn-Ga* systems have led in part to controversial conclusions [30-32]. The aim of this document is to compare the effect of corrosion attack and its possible passivation in polycrystalline ferromagnetic shape memory alloys with different contents of *Fe* in *Ni-Mn-Ga* system and ternary alloy of *Co-Ni-Ga* in aqueous *NaCl* 3.5 wt % solution by cyclic polarization curves.

2. EXPERIMENTAL PROCEDURE

2.1. Preparation of polycrystalline ingots

Polycrystalline ingots of *Fe-Doped Ni-Mn-Ga*, $Co_{38.3}Ni_{32.1}Ga_{29.6}$ and $Ni_{52.7}Mn_{21.9}Ga_{25.4}$ were prepared by arc melting under controlled atmosphere. The alloys were re-melted in order to improve homogeneity four times. The materials used for casting were pure elements *Ni* (99.9%), *Mn* (99.9%), *Ga* (99.99%), *Co* (99.9%) and *Fe* (99.9%), and then some slices were extracted and encapsulated in a

quartz tube for a thermal treatment. Heat treatment was applied at temperature of 800 °C for 72 h and subsequently quenching in water for *Fe-Doped Ni-Mn-Ga* and $Ni_{52.7}Mn_{21.9}Ga_{25.4}$ in order to homogeneity the structure. In the case of $Co_{38.3}Ni_{32.1}Ga_{29.6}$ alloy the treatment was applied to improve homogeneity and structural ordering at temperature of 1100°C for 24 h and 900°C for 24 h then quenching in water. The materials were processing from the ingots by a wire-cutting machine with diamond paste to obtain the necessary area and thus perform the electrochemical tests. Equally the slices were used for complementary analysis.

2.2. Characterization

The alloys were characterized by Differential Scanning Calorimetry (DSC) with a DSC calorimeter Q200 by TA instruments. The using conditions was a ramp of 10 °C / min during heating and cooling, the samples tested were about 20 mg. As can be seen in figure 1, obtained data from cooling and heating of calorimetric runs are shown. Chemical composition of alloys and corrosion deposits were determined Spectroscopy X-ray Energy Dispersive (EDS) technique in JEOL JSM-5800LV equipment. Structure was identified on powder samples at room temperature (for *Fe-Doped Ni-Mn-Ga* alloys) and on bulk samples (for $Co_{38.3}Ni_{32.1}Ga_{29.6}$ alloy) by using an X-ray diffractometer Siemens D5000 with Cu Kα radiation. NaCl powder was mixed with powder of the alloy as a reference for alloys with *Fe-Doped*. Table 1 presents the compositions for each alloy and temperatures of transition. The material was electrical connected using copper wire and spot welded in order to carry out corrosion test, and then each specimen was encapsulated for metallographic preparation. Experiments were carried out on a three-electrode cell of platinum wire as auxiliary electrode, saturated calomel electrode (SCE) as a reference for electrochemical analysis. For the analysis was used a potentiostat galvanostat equipment AUT84861 model. Solution of 3.5 wt% of NaCl was used as electrolyte. Before the experiment of polarization the specimen is immersed for a period of time in the solution in order to stabilizing the system. Results of polarization curves were performed with a scan rate of 0.5 mV/s in a sweep of around -1100mV to 1000mV$_{SCE}$. According to the following equations the corrosion rates were obtained from Rp resistance:

$$CR(mm/year) = \frac{3.27E^{-3}}{\rho} IcorrEw$$

$$(1)$$

$$R_p = \frac{\beta_a \beta_c}{2.303(\beta_a + \beta_c)I_{corr}}$$

$$(2)$$

Where i$_{corr}$ is the corrosion current density (nA/cm^2), Ew is the equivalent weight of calculated alloy according to ASTM G102-89(2010), ρ is the density of the alloy (g/cm^3), Rp is the polarization resistance (Ω-cm^2), ßa and ßc (mV) are the slopes of Tafel plot.

3. RESULTS AND DISCUSSION

The martensitic and austenitic transformation temperatures can be observed in figure 1. Likewise transformation temperatures and compositions obtained in each alloy are shown in table 1. In this context, alloy $Ni_{51.8}Mn_{24.8}Ga_{21.7}Fe_{1.7}$ was found to be in martensitic phase at room temperature; while alloys $Ni_{51.0}Mn_{24.7}Ga_{23.4}Fe_{0.9}$ and $Ni_{51.5}Mn_{22.5}Ga_{23.9}Fe_{2.1}$ are in austenite phase at room temperature.
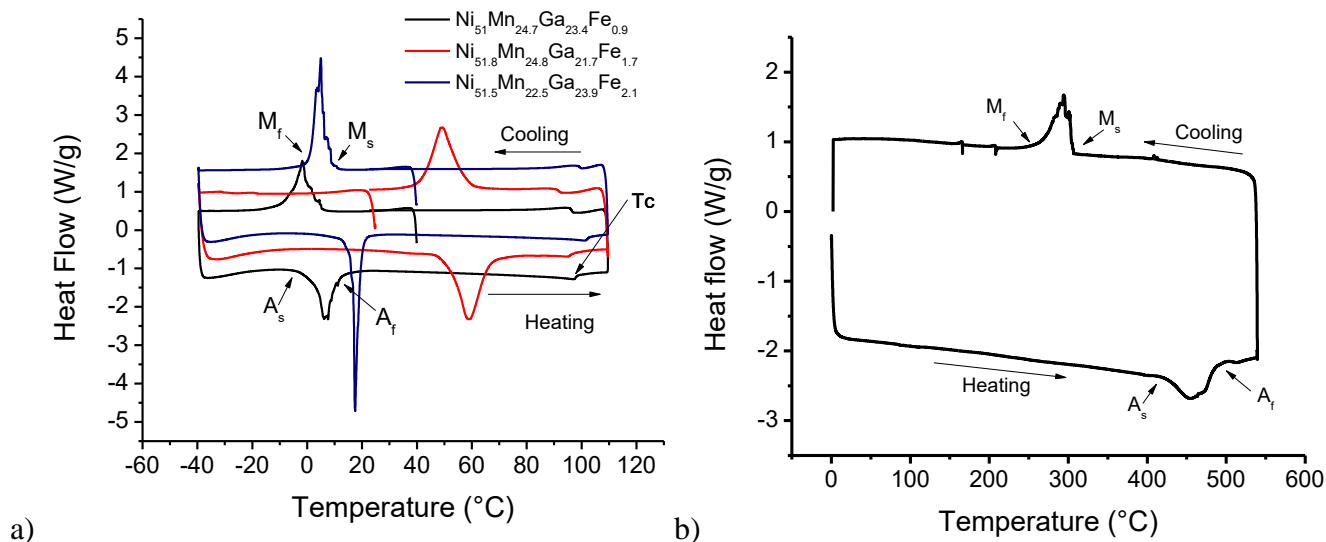

Figure 1. Calorimetric curves from a) the alloys $Ni_{51.0}Mn_{24.7}Ga_{23.4}Fe_{0.9}$, $Ni_{51.8}Mn_{24.8}Ga_{21.7}Fe_{1.7}$ and $Ni_{51.5}Mn_{22.5}Ga_{23.9}Fe_{2.1}$ and b) $Co_{38.3}Ni_{32.1}Ga_{29.6}$ alloy.

In the case of $Co_{38.3}Ni_{32.1}Ga_{29.6}$ alloy shows a martensitic transition at temperature around 300°C and the austenitic transition is 450°C ending around 490°C.

Table 1. Composition and transition temperatures of the alloys studied.

Alloy	Co at.%	Ni at.%	Mn at.%	Ga at.%	Fe at.%	M_s°C	M_f°C	A_s°C	A_f°C
$Ni_{52.7}Mn_{21.9}Ga_{25.4}$	0	52.7	21.9	25.4	0	13.4	4.7	8	17.1
$Co_{38.3}Ni_{32.1}Ga_{29.6}$	38.3	32.1	0	29.6	0	316.9	275.8	450.9	490.3
$Ni_{51.0}Mn_{24.7}Ga_{23.4}Fe_{0.9}$	0	51.0	24.7	23.4	0.9	-0.1	-5.8	1.5	5.3
$Ni_{51.8}Mn_{24.8}Ga_{21.7}Fe_{1.7}$	0	51.8	24.8	21.7	1.7	55.7	41.7	46.1	59.9
$Ni_{51.5}Mn_{22.5}Ga_{23.9}Fe_{2.1}$	0	51.5	22.5	23.9	2.1	6.9	0.8	7.2	15.0

Figure 2 shows a diffraction pattern of the parent phase at room temperature (a) and martensitic phase (b). The diffraction pattern (figure 2a) showed superlattice reflections which correspond to the L2$_1$ Heusler structure in $Ni_{51.5}Mn_{22.5}Ga_{23.9}Fe_{2.1}$. [33]
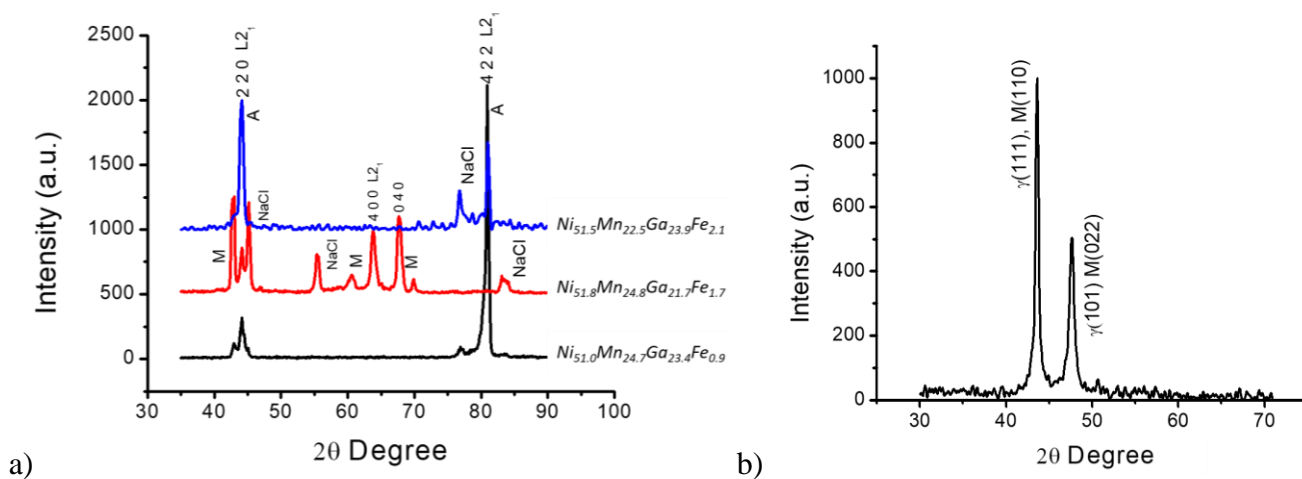
Figure 2. X-ray diffraction pattern for a) $Ni_{51.0}Mn_{24.7}Ga_{23.4}Fe_{0.9}$, $Ni_{51.8}Mn_{24.8}Ga_{21.7}Fe_{1.7}$, $Ni_{51.5}Mn_{22.5}Ga_{23.9}Fe_{2.1}$ and b) $Co_{38.3}Ni_{32.1}Ga_{29.6}$ alloy at room temperature.

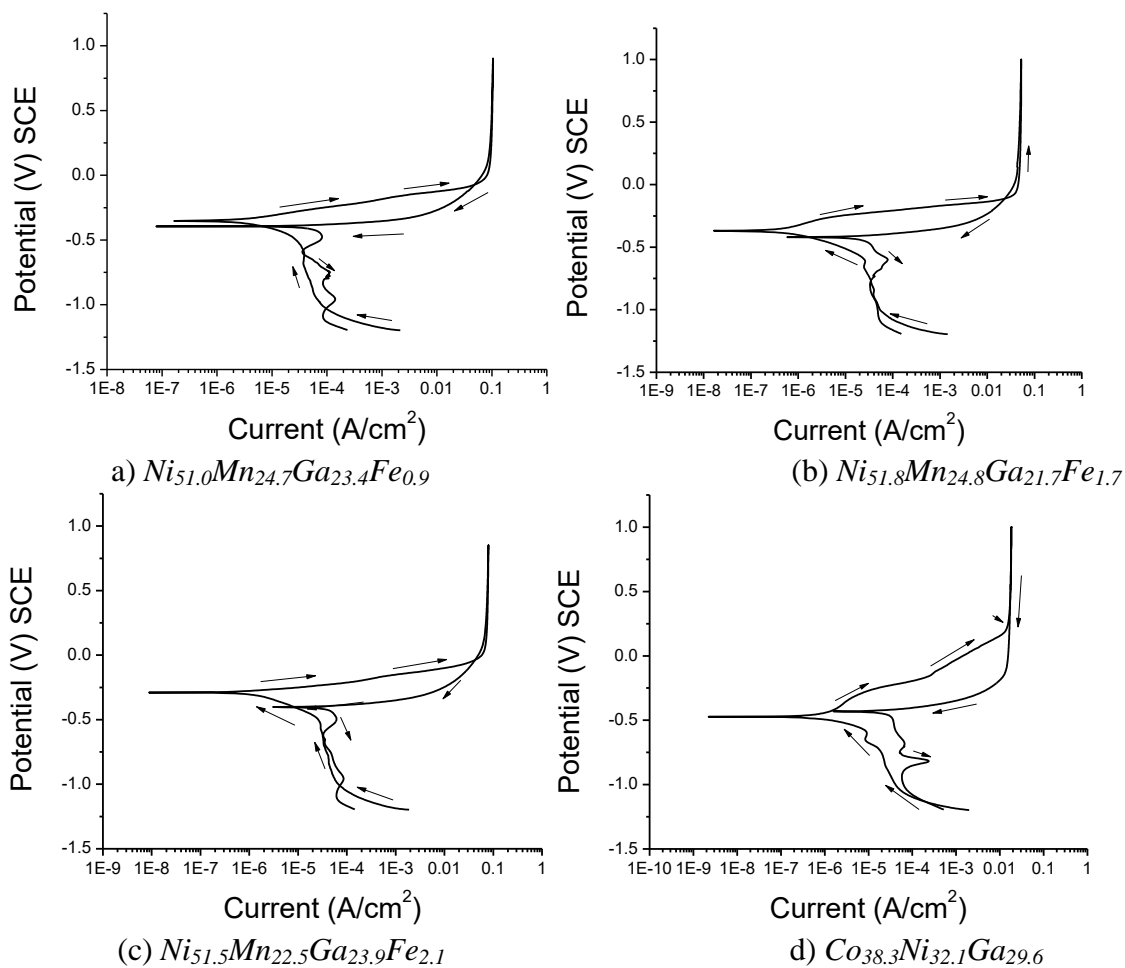## 3.1 Cyclic polarization curves.

Figure 3. Polarization curves obtained, exposed to a 3.5 wt% NaCl solution a)$Ni_{51.0}Mn_{24.7}Ga_{23.4}Fe_{0.9}$, b)$Ni_{51.8}Mn_{24.8}Ga_{21.7}Fe_{1.7}$ and c)$Ni_{51.5}Mn_{22.5}Ga_{23.9}Fe_{2.1}$ and d)$Co_{38.3}Ni_{32.1}Ga_{29.6}$.

Electrochemical characterization of the different alloys were tested in an aqueous solution of 3.5 wt% NaCl, the figure 3 shows the cyclic polarization curves.

From the plots in figure 3, current density values (i_{corr}) and corrosion potential E_{corr} were obtained. Experiments were repeated at least twice, and in all cases the results represent the average value. The table 2 shows the tendency of the i_{corr} in each of the alloys tested, it can be seen that the alloy $Ni_{52.7}Mn_{21.9}Ga_{25.4}$ has the highest i_{corr} and the alloy $Ni_{51.5}Mn_{22.5}Ga_{23.9}Fe_{2.1}$ has a smaller i_{corr}. This implies that the deterioration of the alloy $Ni_{51.5}Mn_{22.5}Ga_{23.9}Fe_{2.1}$ decreased compared to the alloys with lower *Fe* content, in the case of $Co_{38.3}Ni_{32.1}Ga_{29.6}$ alloy shows an i_{corr} compared to that with lower content of *Fe* and also better behavior than the alloy $Ni_{52.7}Mn_{21.9}Ga_{25.4}$.

Table 2. i_{corr} for studied alloys in an electrolyte - 3.5 wt% NaCl.

Alloys	i_{corr} (nA/cm^2)
$Ni_{52.7}Mn_{21.9}Ga_{25.4}$	1678.10
$Co_{38.3}Ni_{32.1}Ga_{29.6}$	347.77
$Ni_{51.0}Mn_{24.7}Ga_{23.4}Fe_{0.9}$	360.90
$Ni_{51.8}Mn_{24.8}Ga_{21.7}Fe_{1.7}$	182.64
$Ni_{51.5}Mn_{22.5}Ga_{23.9}Fe_{2.1}$	150.18

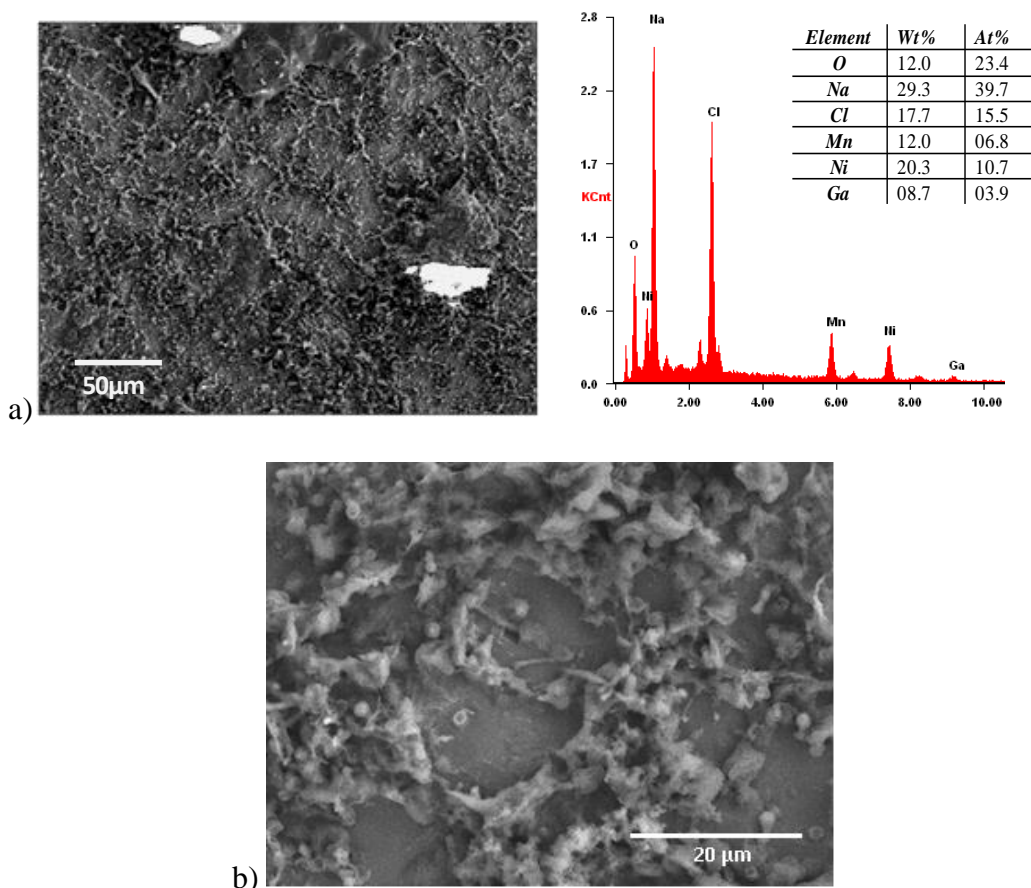| Element	Wt%	At%
O	12.0	23.4
Na	29.3	39.7
Cl	17.7	15.5
Mn	12.0	06.8
Ni	20.3	10.7
Ga	08.7	03.9

a)

b)

Figure 4. a) Images obtained from SEM (200x) and the general EDS result after the electrochemical test for $Ni_{51.0}Mn_{24.7}Ga_{23.4}Fe_{0.9}$ alloy, b) same alloy at 2000x.

From figure 3 it can be seen that the general behavior is active-passive, i.e. showing general dissolution in the process of corrosion, current density is continues increasing up to a certain value presents a spontaneous passive behavior [34]. Gebert et al [35] obtained from electrochemical experiments polycrystalline alloys of the system *Ni-Mn-Ga* from neutrla pH values to alkaline, the tendency of the curves was of spontaneous passivation, under these conditions there was no difference in behavior either austenite or martensite phase. In the case of results showed in figure 3, no transpassivity effect was observed even at high values of potential. This could be attributed to Fe contents for the alloys and also similar behavior was presents for $Co_{38.3}Ni_{32.1}Ga_{29.6}$ alloy, contrary to values obtained by Gebert et al. [35] The results shows a slight transpasivity response around 0.5 volt and neutral pH. Nevertheless it shows in the reverse sweep follows along the same path that could be no tendency to localized corrosion attack to this material. Figure 3 showed a slope of low breakdown potential this could be associated with an increased propagation of localized attack, this is because when is presence a long hysteresis it could be an indicative of localized attack [32].
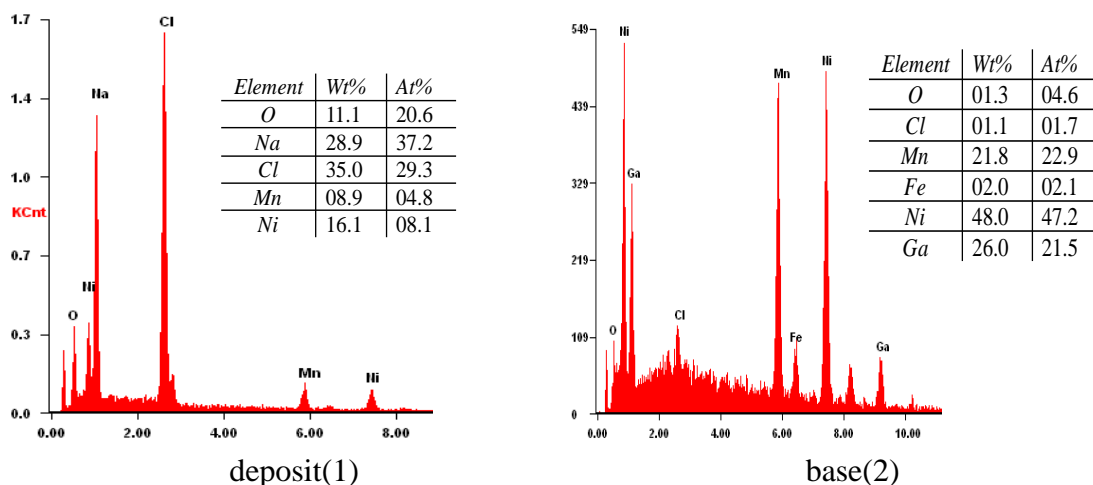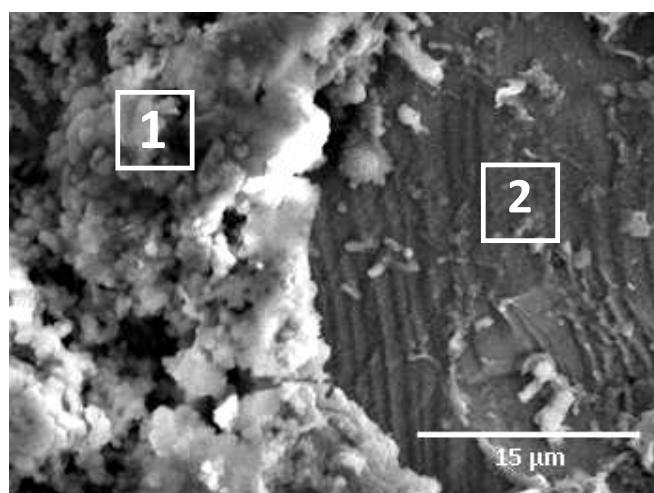

Element	Wt%	At%
O	11.1	20.6
Na	28.9	37.2
Cl	35.0	29.3
Mn	08.9	04.8
Ni	16.1	08.1

deposit(1)

Element	Wt%	At%
O	01.3	04.6
Cl	01.1	01.7
Mn	21.8	22.9
Fe	02.0	02.1
Ni	48.0	47.2
Ga	26.0	21.5

base(2)

Figure 5. Image (3000x) and general EDS results from SEM after electrochemical test for $Ni_{51.8}Mn_{24.8}Ga_{21.7}Fe_{1.7}$ alloy.

After various samples tested (see figure 4 to 7), it is noted that the attack was very aggressive for the material. It is showing a general dissolution attack; while in figure 5, a kind of crater with a reservoir or crusting was observed. Corrosion deposits were more uniform, figure 6, compared to the other cases that is possibly attributed to an increased amount of *Fe*. Figure 4b with fewer *Fe* containing doping, the oxide presents morphology with some flakes shaped deposits and also shows uncovered areas by this product. During the study of the morphology, the material was analyzed by EDS technique to identify the elements present on the corroded surface. Figure 4 has a general EDS where, according to the values, there is an amount of Ni and Mn such as Na, Cl and O that possible cause the corrosion deposit. It can be seen in figure 5 the presence of two zones: with and without a deposit Zone 1 is constituted by deposit is mainly of Na, Cl, Ni and O, with 8% by weight of Mn; while Zone 2 without the presence of deposit is presented higher percentages of Mn, Ni, Ga and lower percentages of Cl, Fe and O how about 1% by weight.

Results were obtained for the $Ni_{51.5}Mn_{22.5}Ga_{23.9}Fe_{2.1}$ alloy, figure 6, indicates that the highest percentage elements present in the analyzed surface were Ga, Na, Ni, Cl, Mn and the lower were Fe and O.
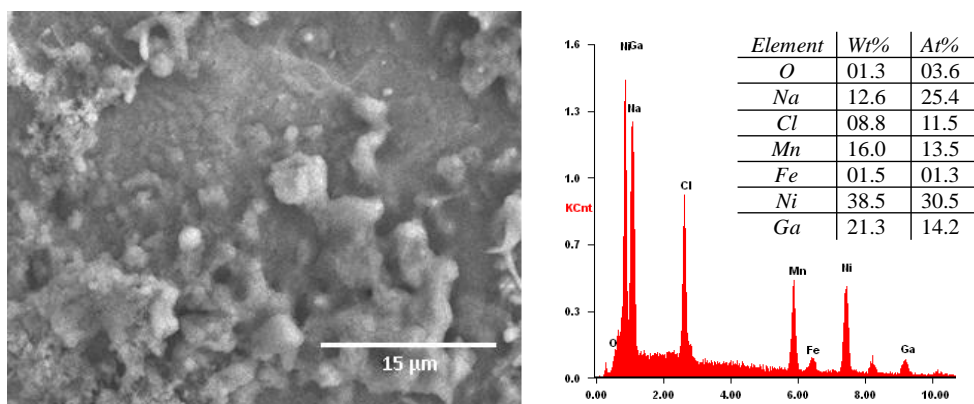

Element	Wt%	At%
O	01.3	03.6
Na	12.6	25.4
Cl	08.8	11.5
Mn	16.0	13.5
Fe	01.5	01.3
Ni	38.5	30.5
Ga	21.3	14.2

Figure 6. Image (3000x) and EDS result from SEM after electrochemical test for the $Ni_{51.5}Mn_{22.5}Ga_{23.9}Fe_{2.1}$ alloy.

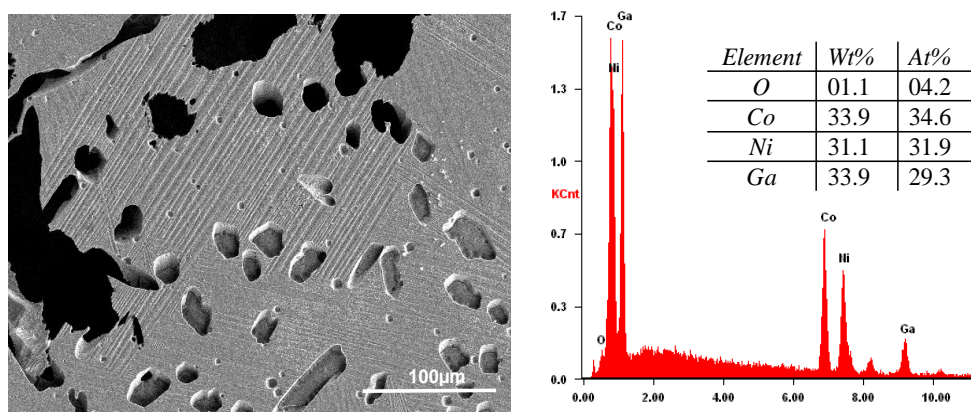| Element	Wt%	At%
O	01.1	04.2
Co	33.9	34.6
Ni	31.1	31.9
Ga	33.9	29.3

Figure 7. Iimage and its corresponding EDS result from SEM after electrochemical test for the alloy $Co_{38.3}Ni_{32.1}Ga_{29.6}$.

The results obtained for the $Co_{38.3}Ni_{32.1}Ga_{29.6}$ alloy shows morphology with some martensitic phase and zones where precipitates were attack selectively, the general EDS, according to the values in the table, shows a substantial amount of Ni and Co suchlike Ga and O. This mean that the presence of O plays an important role in the protection of tested alloys.

4. CONCLUSIONS

From the results obtained, it can be concluded that:

a) The alloys tested in this study i_{corr} decreases with increasing Fe content.

b) $Co_{38.3}Ni_{32.1}Ga_{29.6}$ alloy shows lower i_{corr} than $Ni_{52.7}Mn_{21.9}Ga_{25.4}$ in this media.

c) Elements such as Mn, Ni and Co plus O are present in an important quantity for the corrosion deposits.

d) From polarization curves results, the tested alloys show a general dissolution behavior until certain potential where at certain potential a spontaneous behavior occur.

e) Corrosion deposits were found in alloy $Ni_{51.5}Mn_{22.5}Ga_{23.9}Fe_{2.1}$ with more homogeneity and uniform even though there were some porous, compared to the other cases with *Fe-doped*.

f) For $Ni_{51.0}Mn_{24.7}Ga_{23.4}Fe_{0.9}$ alloy, the corrosion deposit presents morphology of some flakes shaped and also shows uncovered areas possible attributed to slightly lack of adherence.

References

1. K. Ullakko, J. Huang, C. Kantner, R. O'handley, V. Kokorin, *Appl. Phys. Lett.*, 69 (1996) 1966.
2. P. Mullner, V. Chernenko, G. Kostorz, *J. Appl. Phys.*, 95 (2004) 1531.
3. M. Kohl, D. Brugger, M. Ohtsuka, T. Takagi, *Sensors Actuat. A-Phys.*, 114 (2004) 445.
4. N. Sarawate, M. Dapino, *Appl. Phys. Lett.,* 88 (2006) 121923.
5. J. Feuchtwanger, K. Griffin, J. Huang, D. Bono, R.C. O'Handley, S.M. Allen, *J. magn. magn. mater.*, 272 (2004) 2038.
6. O. Söderberg, A. Sozinov, Y. Ge, S.-P. Hannula, V. Lindroos, *Handb. magn. mater.*, 16 (2006) 1.
7. E. Bonnot, R. Romero, L. Mañosa, E. Vives, A. Planes, *Phys. rev. lett.*, 100 (2008) 125901.
8. A. Planes, L. Mañosa, M. Acet, *J. Phys. Condens. Mat.*, 21 (2009) 233201.
9. K.A. GschneidnerJr, V. Pecharsky, A. Tsokol, *Rep. Prog. Phys.,* 68 (2005) 1479.
10. A. Cherechukin, I. Dikshtein, D. Ermakov, A. Glebov, V. Koledov, D. Kosolapov, V. Shavrov, A. Tulaikova, E. Krasnoperov, T. Takagi, *Phys. Lett.* A., 291 (2001) 175.
11. V. Buchelnikov, I. Dikshtein, R. Grechishkin, T. Khudoverdyan, V. Koledov, Y. Kuzavko, I. Nazarkin, V. Shavrov, T. Takagi, *J. magn. magn. mater.*, 272–276, Part 3 (2004) 2025.
12. A.A. Cherechukin, V.V. Khovailo, R.V. Koposov, E.P. Krasnoperov, T. Takagi, J. Tani, *J. magn. magn. mater.*, 258–259 (2003) 523.
13. S. Guo, Y. Zhang, B. Quan, J. Li, Y. Qi, X. Wang, *Smart. mater. struct.*, 14 (2005) S236.

14. V.V. Khovailo, V.A. Chernenko, A.A. Cherechukin, T. Takagi, T. Abe, *J. magn. magn. mater.*, 272–276, Part 3 (2004) 2067.

15. D. Kikuchi, T. Kanomata, Y. Yamaguchi, H. Nishihara, K. Koyama, K. Watanabe, *J. Alloy. Compd.*, 383 (2004) 184.

16. K. Koho, O. Söderberg, N.a. Lanska, Y. Ge, X. Liu, L. Straka, J. Vimpari, O. Heczko, V. Lindroos, *Mater. Sci. Eng.* A., 378 (2004) 384.

17. Z. Liu, M. Zhang, W. Wang, W. Wang, J. Chen, G. Wu, F. Meng, H. Liu, B. Liu, J. Qu, *J. appl. phys.*, 92 (2002) 5006.

18. G. Wu, W. Wang, J. Chen, L. Ao, Z. Liu, W. Zhan, T. Liang, H. Xu, *Appl. Phys. Lett.*, 80 (2002) 634.

19. R.D. James, M. Wuttig, *Philos Mag.* A., 77 (1998) 1273.

20. T. Kakeshita, T. Takeuchi, T. Fukuda, T. Saburi, R. Oshima, S. Muto, K. Kishio, *JIM, Mater. Trans.*, 41 (2000) 882.

21. F. Gejima, Y. Sutou, R. Kainuma, K. Ishida, *Metall. Mater. Trans.* A., 30 (1999) 2721.

22. K. Oikawa, L. Wulff, T. Iijima, F. Gejima, T. Ohmori, A. Fujita, K. Fukamichi, R. Kainuma, K. Ishida, *Appl. Phys. Lett.*, 79 (2001) 3290.

23. H. Morito, A. Fujita, K. Fukamichi, R. Kainuma, K. Ishida, K. Oikawa, *Appl. Phys. Lett.*, 81 (2002) 1657.

24. S. Kaul, B.A. D'Santhoshini, A. Abhyankar, L.F. Barquin, P. Henry, *Appl. Phys. Lett.*, 89 (2006) 093119.

25. K. Oikawa, T. Ota, F. Gejima, T. Ohmori, R. Kainuma, K. Ishida, *Mater. Trans. JIM.,* 42 (2001) 2472.

26. R. Kainuma, M. Ise, C.-C. Jia, H. Ohtani, K. Ishida, *Intermetallics.*, 4 (1996) S151.

27. A. Tejeda-Cruz, F. Alvarado-Hernández, D. Soto-Parra, R. Ochoa-Gamboa, P. Castillo-Villa, H. Flores-Zúñiga, S. Haro-Rodriguez, A. Santos-Beltrán, D. Ríos-Jara, *J. Alloy. Compd.*, 499 (2010) 183-186.

28. R. Kainuma, S. Imano, H. Ohtani, K. Ishida, *Intermetallics.*, 4 (1996) 37-45.

29. T. Omori, N. Kamiya, Y. Sutou, K. Oikawa, R. Kainuma, K. Ishida, *Mater. Sci. Eng. A. struct.*, 378 (2004) 403.

30. X. Liu, O. Sôderberg, Y. Ge, N. Lanska, K. Ullakko, V. Lindroos, J. Phys. IV., (Proceedings), EDP sciences, 2003, pp. 935.

31. A. Sozinov, O. Söderberg, V. Lindroos, Y. Ge, X.W. Liu, Mater. Sci. Forum., *Trans Tech Publ*, 2002, pp. 565.

32. L. Stepan, D. Levi, E. Gans, K. Mohanchandra, M. Ujihara, G. Carman, *J. Biomed. Mater. Res.* A., 82 (2007) 768.

33. D. Soto-Parra, F. Alvarado-Hernandez, O. Ayala, R. Ochoa-Gamboa, H. Flores-Zuniga, D. Rios-Jara, *J. Alloy. Compd.*, 464 (2008) 288.

34. B. Guo, Y. Tong, F. Chen, Y. Zheng, L. Li, C. Chung, *Mater.Corros.*, 63 (2012) 259.

35. A. Gebert, S. Roth, S. Oswald, L. Schultz, *Corros. Sci.*, 51 (2009) 1163